Postseismic Survey of a Historic Masonry Tower and Monitoring of Its Dynamic Behavior in the Aftermath of Le Teil Earthquake (Ardèche, France)

Andy Combey, E. Diego Mercerat, Philippe Gueguen, Mickaël Langlais, Laurence Audin

BSSA (10.1785/0120210258)

Postseismic survey of a historic masonry tower and monitoring of its dynamic behaviour in the aftermath of Le Teil earthquake (Ardèche, France).

Andy Combey[a]*, E. Diego Mercerat[b], Philippe Gueguen[a], Mickaël Langlais[a] and Laurence Audin[a]

[a] Univ. Grenoble Alpes, Univ. Savoie Mont Blanc, CNRS, IRD, UGE, ISTerre, 38000 Grenoble, France
[b] CEREMA, Repsody team, Sophia Antipolis, 06360 Valbonne, France

*To whom correspondence may be addressed:
Andy Combey, ISTerre UGA, 1381 Rue de la Piscine, 38610 Gières, France
Email: andy.combey@univ-grenoble-alpes.fr

Keywords

Masonry Towers; Random Decrement Technique; Vibration sources; Nonlinear dynamics; Le Teil earthquake

Abstract

On November 11th, 2019, a Mw 4.9 earthquake struck the middle Rhône valley (South-East France) producing moderate to severe damage in the town of Le Teil and its surroundings. This unexpected event stressed the vulnerability of the French cultural built heritage to a moderate seismic hazard. Commonly applied to modern civil engineering structures, passive seismic methods are still lacking on historic constructions to understand properly the different factors driving their dynamic behaviour. In this paper, the results of a two-month seismic monitoring survey carried out shortly after the Le Teil mainshock in a historic masonry tower are presented and discussed. Located only 5 km south of the epicentre, the Gate Tower of Viviers (11th century) was instrumented with four highly sensitive seismic nodes. Ambient vibrations, as well as aftershocks and quarry blasts from the nearby Le Teil quarry, were recorded and used in the analysis. Through vibration-based analysis, the paper addresses three relevant aspects of the dynamic response of ancient masonry structures. We discuss first the differences in the building's response induced by the three reported types of vibrations, focusing on the particular signal characteristics of shallow aftershocks and quarry blasts. Then, we apply the Random Decrement Technique (RDT) to track the dynamic behaviour variations over two months and to discuss the role of the environmental conditions in the slight fluctuations of the structural modal parameters (natural frequencies, damping coefficients) of unreinforced masonry structures. We also show evidence of the non-linear elastic behaviour under both weak seismic and atmospheric loadings. The correlation between the presence of heterogeneities in the

construction materials and the non-linear threshold supports the relevance of such types of monitoring surveys as a valuable tool for future modelling works and conservation efforts.

1. Introduction

Characterizing the dynamic response of buildings under a wide range of stresses and loadings has turned into a key component of structural health monitoring (SHM) and condition-based maintenance studies. Cost-effective and easy to implement, operational modal analysis (OMA) constitutes the starting point to any SHM or damage assessment. These approaches rely on the basic principle that any modification of the building's operational dynamic response indicates a modification of the stiffness or energy dissipation characteristics of the system, since the masses are assumed not to change (Farrar and Worden, 2007). Applied to civil engineering structures (e.g., bridges, towers, buildings, etc.) ambient vibration-based techniques provide an accurate assessment of modal parameters (frequency, damping, mode shapes) for health monitoring.

Regarding cultural heritage buildings, the complexity of their architecture coupled with their successive construction phases makes operational interpretations particularly difficult for the SHM. This limits the implementation of effective preservation strategies, while their vulnerability to dynamic and cumulative loads is amplified by their current structural health status (Cabboi et al., 2017; Korswagen et al., 2020). Often slender and heavy, tall historic structures are particularly vulnerable to earthquakes. Assessing and modelling their seismic performance has become thus a growing priority of Heritage safeguarding strategies (Jaishi et al., 2003; Dogangun et al., 2008; Clemente et al., 2015; Ronald et al., 2018; Micelli and Cascardi, 2020). Studying masonry buildings with a cultural heritage value implies nonetheless dealing with additional regulatory and technical constraints. In such cases, the implementation of non-invasive and non-disturbing techniques such as passive seismic methods are particularly suitable and recommended (Gentile and Saisi, 2007; Ceravolo et al., 2016). Besides instrumentations of emblematic monuments (Pau and Vestroni, 2008; Hinzen et al., 2012; Lacanna et al., 2016) and bridges (Azzara et al., 2017; Roselli et al., 2018), recent works on Italian historic masonry towers (e.g., Cabboi et al., 2017; Ubertini et al., 2017; Saisi et al., 2018; Azzara et al., 2019; Barsocchi et al., 2020) demonstrated the relevance of those approaches for conservation purposes.

Material heterogeneities and pre-existing cracks play also a significant role in the dynamic response of structures. Guéguen et al. (2016, 2020) and Astorga et al. (2018, 2019) extrapolated the micro-scale nonlinear elasticity studies applied to rock samples (e.g., Johnson and Sutin, 2005) to large-scale reinforced concrete structures in relation to the damage level. Brossault et al. (2018) estimated the damping fluctuation under small deformation as a proxy of the number

of heterogeneities at different scales. Based on both fluctuation-dissipation and nonlinear elasticity theories, the extension of cracks within the masonry may affect notably the variations of modal parameters on quasi-static or moderate dynamic loadings. Despite the uncertainties related to the estimation of the absolute damping value, long-term ambient vibration-based monitoring in historic monuments is, therefore, an efficient way for assessing possible degradation of buildings' elastic properties and structural health.

The Mw 4.9 Le Teil earthquake occurred on November 11, 2019 in the middle Rhône valley (Ardèche, France). The area is well known for its numerous industrial facilities and its rich cultural heritage. The earthquake was particularly shallow (hypocentral depth less than 2 km) and damaging (Cornou et al., 2020; Ritz et al., 2020; Causse et al., 2021). Almost 1,000 houses were severely affected in and around the city of Le Teil. Since the earthquake, monuments with great heritage value such as the church of Mélas and the castle of Saint Thomé (Fig.1) have required important retrofitting efforts. Besides the severe lack of knowledge on the local seismic hazard (Mazzotti et al., 2020; Naud, 2021), the event highlighted hence the seismic vulnerability issue of the local cultural heritage. Due to this "historically unprecedented earthquake in France" (Ritz et al., 2020), the region has turned into a testing ground for numerous research projects focused on the French seismic hazard assessment and the seismic monitoring of civil engineering structures.

This event provided a rare opportunity to monitor a historic masonry building during a post-seismic sequence in France and to use both ambient and transient dynamic vibrations (aftershocks as well as blasts from the open-pit cement quarry of Le Teil). We conducted thus a two-month monitoring of the eleventh-century Gate Tower of Viviers (GTV) located 5 km southeast of the November 11, 2019 epicentre (Fig.1). Apart from the characterization and monitoring of the dynamic behaviour of the GTV, the objective of this work is to identify the main factors driving the elastic response of such a complex and heterogeneous masonry structure in the framework of the seismic vulnerability assessment of historical monuments. This paper examines first the response of the GTV to several aftershocks and blasts from the open-pit cement quarry of Le Teil. Then, we analyse the long-term wandering of the modal frequencies and damping ratio using the Random Decrement Technique (RDT), related to the environmental conditions. Finally, based on the damping assessment, the nonlinear elastic behaviour is interpreted and discussed in terms of SHM. It could be a valuable baseline for future SHM studies dedicated to old masonry monuments.

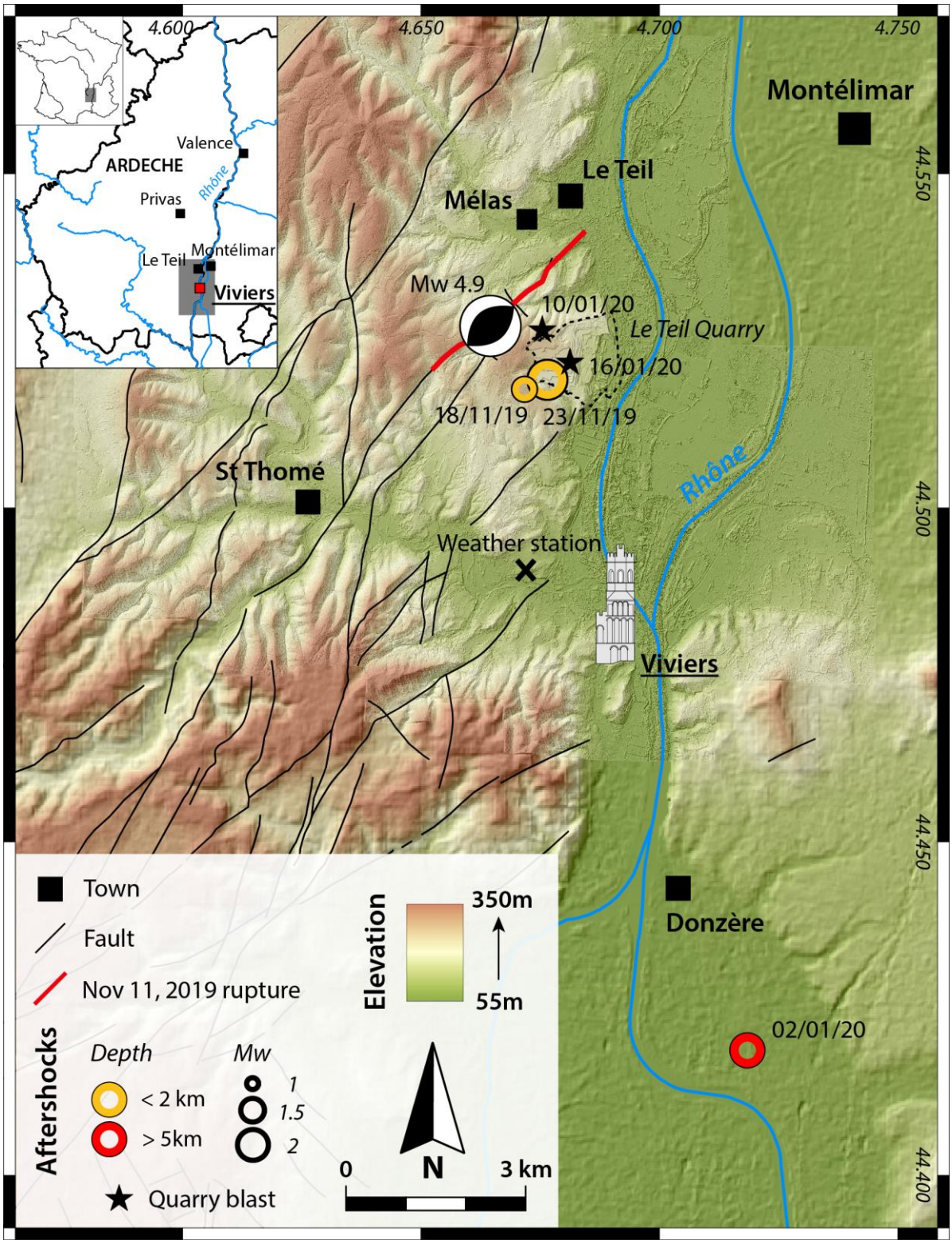

Fig.1 The Viviers-Le Teil area lies in the middle Rhône valley, in the department of Ardèche, France (see inset). The Gate Tower of Viviers (GTV) is located 5 km south of the fault rupture associated with the Mw 4.9 Le Teil earthquake. The location of the main seismic events (coloured circles) and quarry blasts (black stars) discussed in this paper is indicated.

2. The experiment

2.1. The Gate Tower of Viviers

The GTV forms part of the medieval episcopal quarter of Viviers (Fig.2) and reaches a height of 37 meters. The building is listed by the French authorities as a historic monument since 1906. Most likely built in the second half of the 11th century (Esquieu, 1983), preceding thus the construction of the adjoining cathedral, the GTV was initially designed as a monumental and "ostentatious" gate (Esquieu and Guild, 1992) giving access to the episcopal area on the rocky hill of Viviers. Located at the eastern edge of the Urgonian (Early Cretaceous) massif (Elmi et al., 1996), the calcareous outcrop forms a high point segregating naturally the cathedral complex from the rest of the town (Fig.2). In the second half of the 12th century, the GTV was raised up, by approximately 10 meters, to serve as the bell tower of the actual cathedral. It is probably during the 14th century and the remodelling works of the Gothic period that a rib vault was constructed on the western porch of the cathedral, connecting tenuously the previous building to the GTV (Esquieu and Guild, 1992 - Fig.3). Around 1387, in a context of political tensions and conflicts (Hundred Years' War), the elites of Viviers decided to raise the top of the tower with an important octagonal floor with crenelated walls (Esquieu and Guild, 1992). Since then, the GTV also played a defensive role and became a strategic vantage point of the Rhône valley. Aside from light retrofitting works during the 19th century, the GTV has undergone few changes since the Middle Ages (Esquieu and Guild, 1992).

The building is, therefore, the result of several constructive phases with a great variety of architectural styles that exemplifies its current heritage value. Constructed in Roman style, the quadrangular base of the Tower reaches a height of approximately 27 meters. It is composed of three levels: a lower room (ground floor) surmounted by a vaulted chapel and a second floor, which was designed to host the bells (Fig.3b). Almost square in plan (9.3 x 9m), the Tower is flanked on its western façade by a large buttress wall, 17 meters high, which ends in a terrace accessible from the second floor (Fig.3). The Tower is entirely built with limestone rocks and local molasses (Esquieu, 2021, pers.comm.). The stonework is relatively poor, characterized by irregular courses and locally thick mortar joints (Esquieu and Guild, 1992 – Fig.3c). Nonetheless, the upper part, octagonal in shape, differs from the base by the common use of ashlars (Fig.3d), preferred to the rubbles used in the lower part.

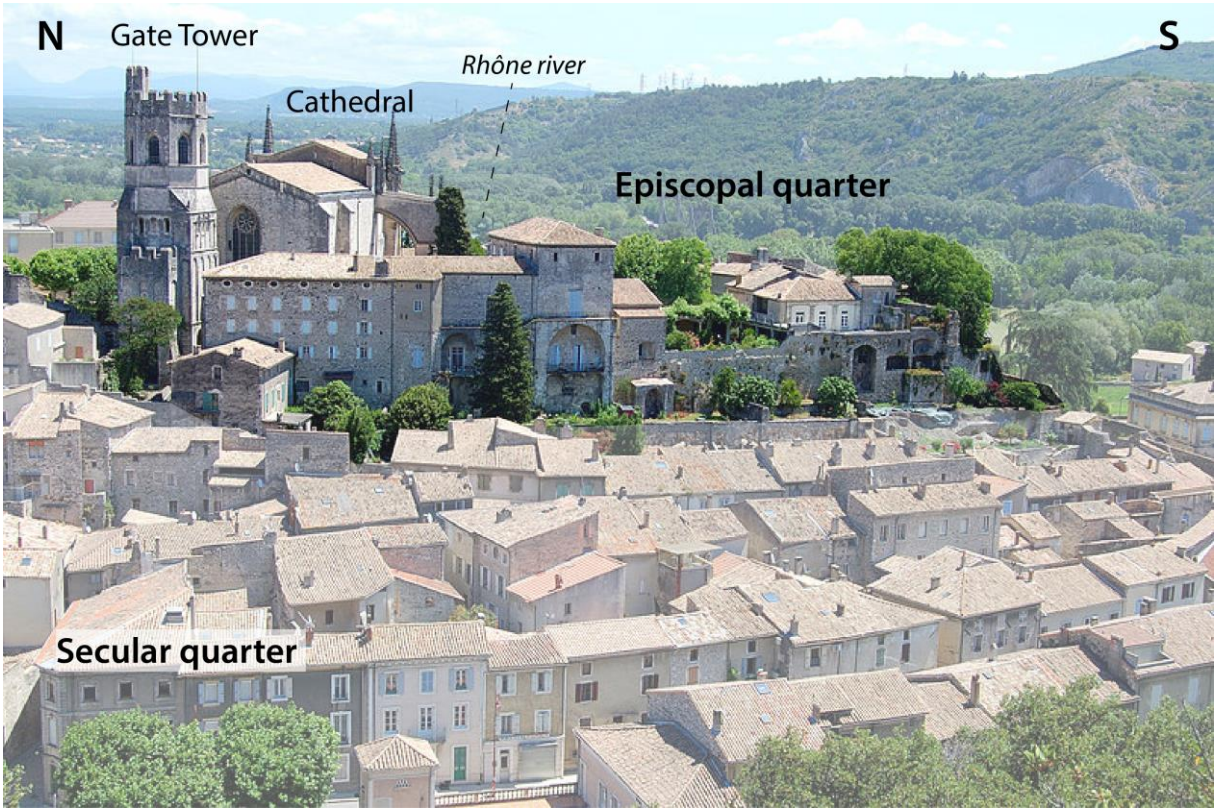

Fig.2 View of Viviers historic centre. Note the strategic location of the episcopal quarter that settles on the edge of a calcareous outcrop, overlooking the middle Rhône valley. The Tower was the main access to this sector during the medieval period.

Notable historical events seem to have affected the nine centuries-old building but without jeopardizing its integrity. It survived the ransacking and looting of Viviers by the Huguenots in 1567 (Esquieu and Guild, 1992) and the fire that affected the cathedral in 1772 (Esquieu, 1988). From the natural hazard point of view, the violent seismic swarm that damaged the Tricastin area in 1873 (MSK intensities VI-VII) and several architectonical features of the cathedral of Viviers (SisFrance database), does not seem to have caused serious damage to the Tower. Regarding the impact of the Le Teil earthquake, a visual inspection three days after the mainshock did not reveal any structural damage in the GTV. However, several pre-existing fractures were re-opened according to the presence of fresh plaster on the chapel's floor.

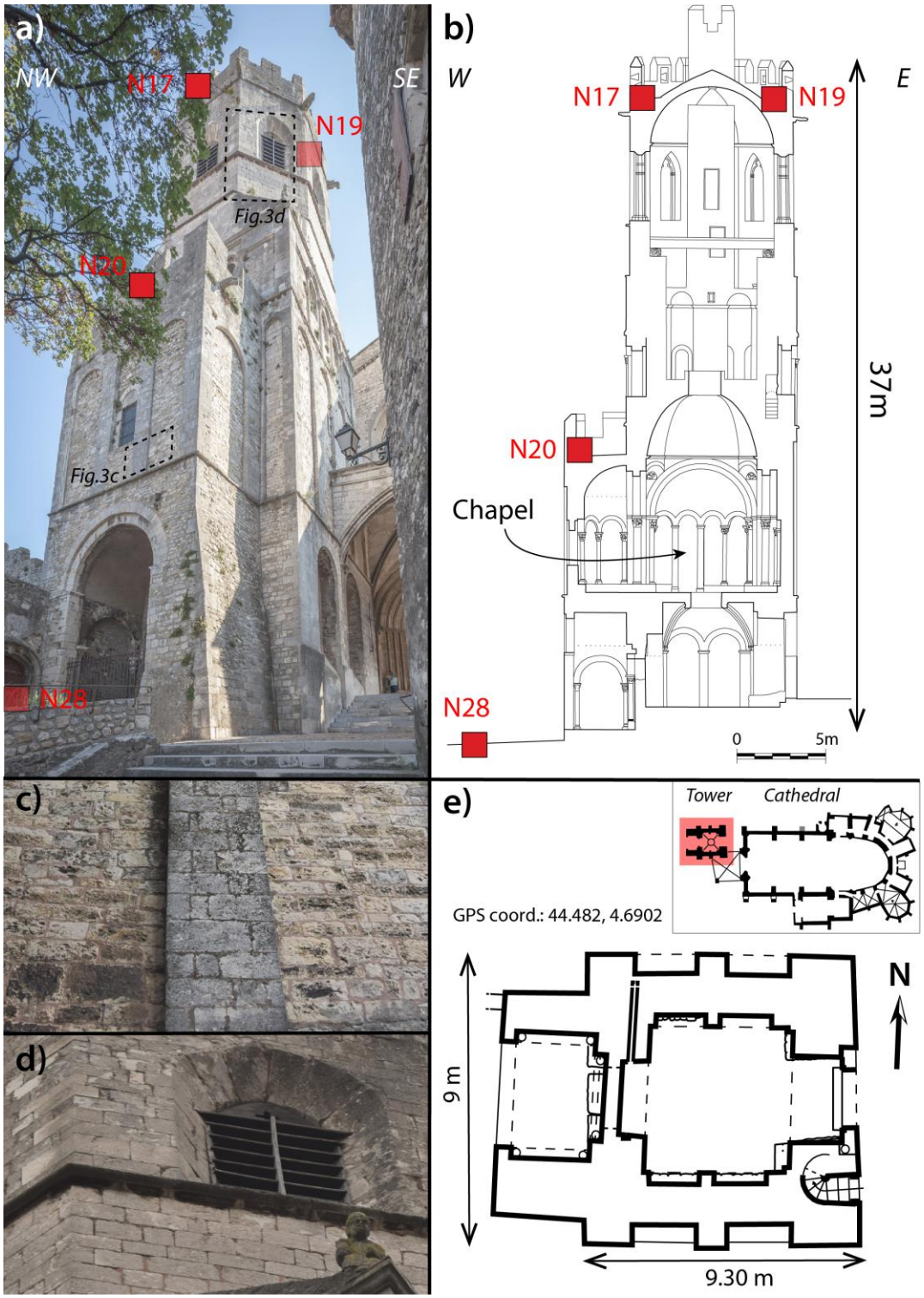

Fig.3 The Gate Tower of Viviers. a) Overview of the building from the entry staircase (southwest) leading to the episcopal sector (credits: X. Spertini); b) Sectional drawing of the building (Esquieu and Guild, 1992); c) Stonework at the first floor. Note the poorly cut stones with thick mortar joints on the left and right parts of the photograph; d) Detail of the ashlar masonry characterizing the upper part of the Tower; e) Plan view of the Tower as well as its location with respect to the cathedral. The red squares indicate the location of the sensors.

2.2. The postseismic survey

Following the shallow and damaging November 11, 2019 Le Teil earthquake and its disastrous impact on local traditional housing and surrounding historical monuments, we carried out a two-month monitoring of the GTV, through the installation of four Fairfield ZLand nodes. The simple geometry of the Tower facilitated its instrumentation with a reduced number of seismic stations. Compact, the nodes included in the same device three geophones (three component velocimeters), a digitizer (24 bits) and a Global Positioning System (GPS). The sensors integrated into the nodes have a nominal sensitivity of 76.7 V/m/s and were configured to a sampling rate of 250 Hz. Operating on battery power, the nodes have approximately 35 days of autonomy.

The instrumentation started seven days after the mainshock with the aim of recording the aftershocks sequence. Four nodes were installed between November 18, 2019 and December 11, 2019, and then replaced by four new instruments until January 17, 2020 to avoid the power issue. For GPS synchronization, those sensors require to be settled in open sky to be operational. This requirement conditioned the location of the nodes within the structure (Fig.3). N28 was installed at the basement of the tower, half-buried on the western side and was used as a reference ground station. N20 was installed at the western extremity of the terrace located between the first and the second floor of the tower and corresponding to the top of the buttress wall. The vertical position of N20 (relative to N28) is approximately 17 meters. Finally, two stations were installed at the top of the tower (N17 and N19), 37 meters above the ground, respectively at the west and east side of the structure. As shown in Figure 3, N28, N20 and N17 were located on the same vertical axis. All the sensors were oriented to the magnetic North. Due to the alignment of the walls of the GTV with the cardinal points (Fig.3), we decided to liken the building's mode shapes in the two horizontal components as purely E-W and N-S motions. Following the FDSN nomenclature, we used the acronyms "DPE", "DPN" and "DPZ" to name the three channels of each geophone, corresponding respectively to the E-W, N-S and vertical components.

On November 11, 2019, the Mw 4.9 Le Teil earthquake was associated with the reactivation of a large part of the NE-SW La Rouvière normal fault in reverse motion (Ritz et al., 2020). A small number of aftershocks followed this moderate-sized but very shallow event that induced a 4.5 km long surface rupture (in red on Fig.1). The dense temporary network of 52 seismological stations deployed in the field only a few days after the mainshock (Cornou et al., 2020) recorded 84 weak-to-moderate earthquakes, with 17 events with a magnitude > 1. During

this sequence, only three events induced a clear response of the GTV and are considered in this paper (Tab.1). The earthquake that occurred on January 02, 2020 was located to the south of the epicentral region (Fig. 1) and was not considered as an aftershock. We succeeded in recording on January 10 and January 16, 2020 the two first quarry blasts triggered in the nearby Le Teil quarry after the mainshock (Fig.1-Tab.1).

The recording of seismic events and quarry blasts during the monitoring of the GTV is of great interest for the study of the Tower's dynamic behaviour. Such data allow discussing the impact of moderate transient shakings on the elastic properties of historic masonry buildings.

Time	Latitude	Longitude	Depth (km)	Magnitude (M_w)	Location	Type
2019-11-18 T12:56:16.69831	44.518852	4.674751	1.60	1.63	VIVIERS	Earthquake
2019-11-23 T22:14:54.787128	44.519180	4.676490	1.48	2.78	VIVIERS	Earthquake
2020-01-02 T17:51:05.490607	44.418732	4.718434	5.06	2.26	DONZERE	Earthquake
2020-01-10 T10:08:48.897093	44.526299	4.674372	0.0	1.78	LE TEIL	Quarry blast
2020-01-16 T10:13:34.975305	44.521587	4.680440	0.0	1.54	LE TEIL	Quarry blast

Table 1 Main information on the five events investigated in the framework of this paper. Their estimated locations are reported in Fig.1.

3. Results and Discussion

3.1. Dynamic behaviour analysis

We analysed 1,426 hours of continuous data recorded by the GTV temporary array, except between 9.30 and 10.00 am on December 11, 2019 for maintenance. All the data and metadata from the post-seismic survey in Viviers were obtained from the Résif-EPOS portal (see Data and Resources Section).

Using the ObsPy package for seismological signal processing, we deconvolved first the instrument's response from the raw signals. Then the OMA was performed using MACity software developed by Michel et al. (2010) using the Frequency Domain Decomposition (FDD) for modal shape assessment (Brincker et al., 2001) based on the singular value decomposition (SVD) of the cross-spectral power density matrix.

Six clear frequency modes were identified in the range 0-15 Hz (Fig.4a-b), associated with six mode shapes of the structure (Fig.4c). The first two peaks at 2.332 Hz (f_{N1}) and 2.698 Hz (f_{E1}) correspond to the first bending modes in the N-S and E-W horizontal components, respectively. Similarly, we identified the second N-S and E-W bending modes at 7.104 (f_{N2}) and 7.617 Hz (f_{E2}), respectively. Two other modes were detected, one torsional mode at 5.615 Hz (f_{T1}) and one vertical mode (f_{V1}) at approximately 12.5 Hz. The sixth vibration mode f_{V1} is associated with a dominant motion in the vertical component (Fig.4c-5), which explains its denomination as a "vertical mode." Such modes are only rarely identified with passive seismic techniques (Lacanna et al., 2016; Ronald et al., 2018) due to the small contribution of this mode under ambient vibrations. OMA indicate relatively high modal frequencies for a 37-meter-high structure compared to empirical relations obtained for masonry towers (Zanotti Fragonara et al., 2017) and argue for a relatively stiff behaviour of the monument.

Besides the squared shape of the Tower, structural elements may induce differences in stiffness within the building and consequently distinct frequencies for both orthogonal bending modes. Frequencies of the bending modes in the N-S direction are lower than in the E-W direction (Fig.4), arguing for the stiffening contribution of the buttress wall on the western façade as well as the rib vault connecting the Tower to the cathedral to the east. The relation between the two first bending modes in the same components indicates behaviour close to that of a shear beam ($f_n=(2n-1)*f_1$ – Fig.4). For that reason, we considered the potential coupling of the GTV with the adjoining cathedral as not significant.

The GTV and the entire episcopal area are settled on a calcareous outcrop. We carried out H/V measurements (Nakamura, 1989) at the bottom of the Tower and two places located a few hundred meters north of the monument. The H/V spectral ratios are similar and display nearly flat spectra between 0.5 and 12 Hz (Fig.5a) that confirms no significant lithological site effects and weak soil-structure interaction.

Transfer functions computed by deconvolution between the top and the bottom of the building have proven to be a useful method to quantify the excitation level of the vibration modes and identify changes in the resonant frequencies resulting from modifications of the building mechanical properties (e.g., Todorovska, 2009). We first calculated the spectral ratio between N17 (full height) and N28 (base) and between N20 (half-height) and N28 (base) on a two-hour window of ambient vibrations. We applied then the same methodology on shorter time windows of 40 seconds using the three seismic events (Tab.1).

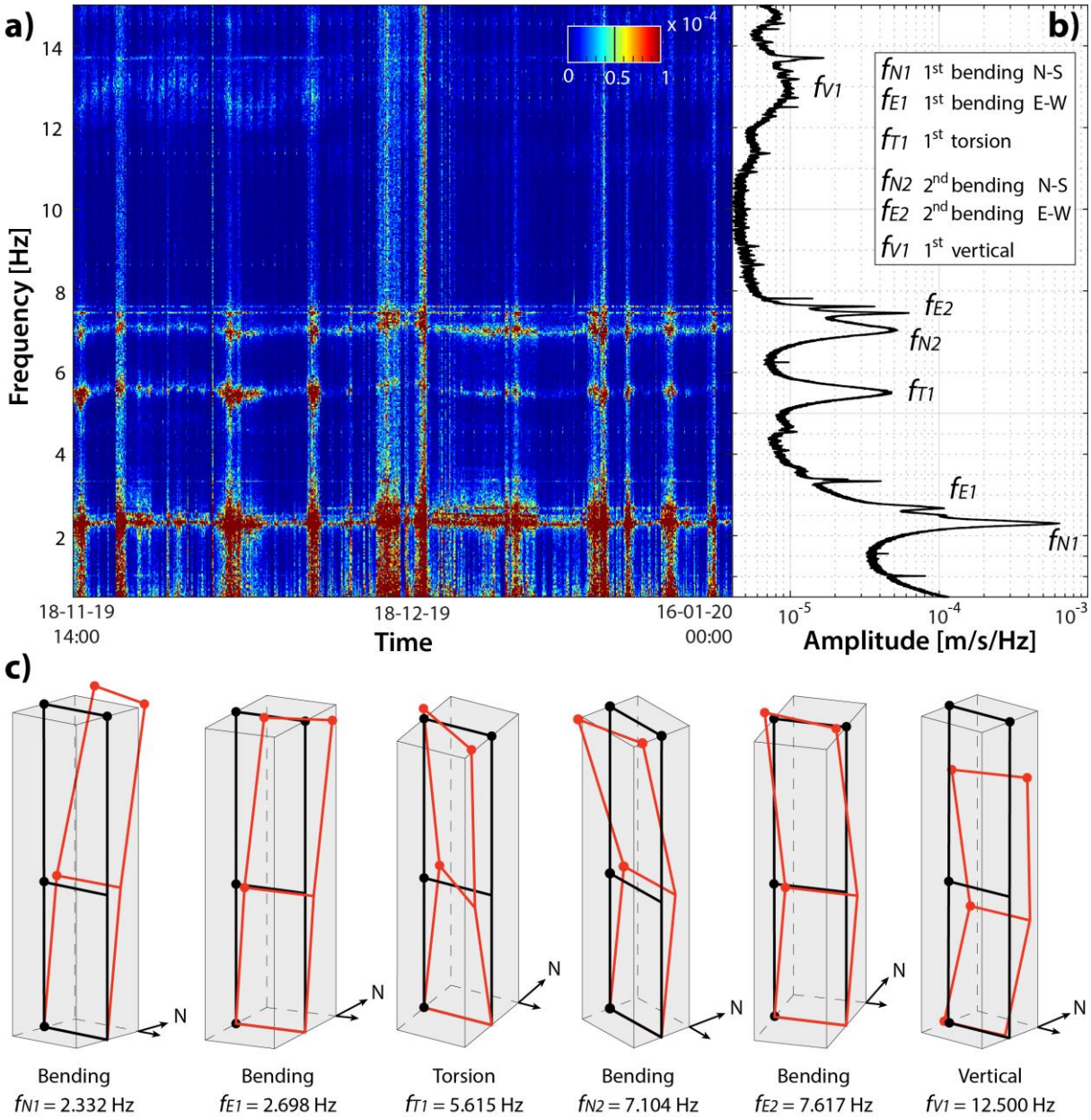

Fig.4 a) N19 spectrogram calculated in the bandwidth 0.5-15 Hz for the period ranging from Nov. 18, 2019 to Jan. 16, 2020; b) Resonant frequencies of the GTV derived from the mean amplitude spectrum; c) The six associated mode shapes. The red frames represent the motion of the vibration mode compared to the static position displayed in black. Nexus points indicate the location of the four velocimeters.

The spectral ratios using ambient vibrations and computed between the top and the bottom of the building (Fig.5b) highlight several important results. The amplitudes of both bending modes are nearly identical in the N-S direction (f_{N1} and f_{N2}) while the amplitude of the second bending mode in the E-W direction (f_{E2}) is more than two times higher than the amplitude of the first one (f_{E1}). The torsion mode (f_{T1}) is slightly excited under ambient vibrations. Barely visible in

the E-W component, the amplitude of the torsion mode only accounts for ~10% of the first bending mode in the N-S component. It is worth pointing out that the amplitude of the vertical mode can be significant under ambient vibrations. Moreover, the spectral ratio between N20 (half-height) and the base (in red in Fig.5b) is significantly different from those obtained between the top and the bottom of the Tower. The amplitude ratio of f_{T1} is larger on the lower part of the building, supporting a non-regular behaviour of the torsional motion throughout the structure. Likewise, the second bending mode in the E-W direction (f_{E2}) mainly occurs at the bottom of the structure that suggest a significant impact of the dissimilar geometry characterizing the base (square) and the top (octagonal) of the GTV (Fig.2-3).

Notwithstanding their moderate magnitudes, their similar distance from the Tower and the equivalent azimuths between the sources and the building (Fig.1-Tab.1), the five transient events induce different responses of the GTV (Fig.6). Regarding first the seismic events, only small differences compared to ambient loading are observed. Figure 7 shows the results of the spectral ratios performed between the top and the base of the building for the three events. In all cases, the two bending modes (amplitude ratio >10) have a larger amplitude compared to Fig.5b. While in the N-S direction amplitude ratios between f_{N1} and f_{N2} are the same as using ambient vibrations, the first bending mode in the E-W component is more excited, similarly to the second bending mode (Fig.7). Surprisingly, the torsion mode appears to be not significantly excited. The response of the GTV during the January 02, 2020 event shows significant differences. Unlike the two other events, the first bending mode is preferentially excited in the E-W direction (Fig.6a-7). Moreover, the amplitudes of the second bending modes in the three components are lower, especially in the E-W direction as f_{E2} represents only a third of the amplitude of f_{E1}. The signal recorded on January 02, 2020, was not related to the post-seismic sequence of the Le Teil earthquake. The differences are, thus, most probably due to the distinct source parameters and focal mechanisms of the third seismic event (Fig.1-Tab.1-Fig.S1).

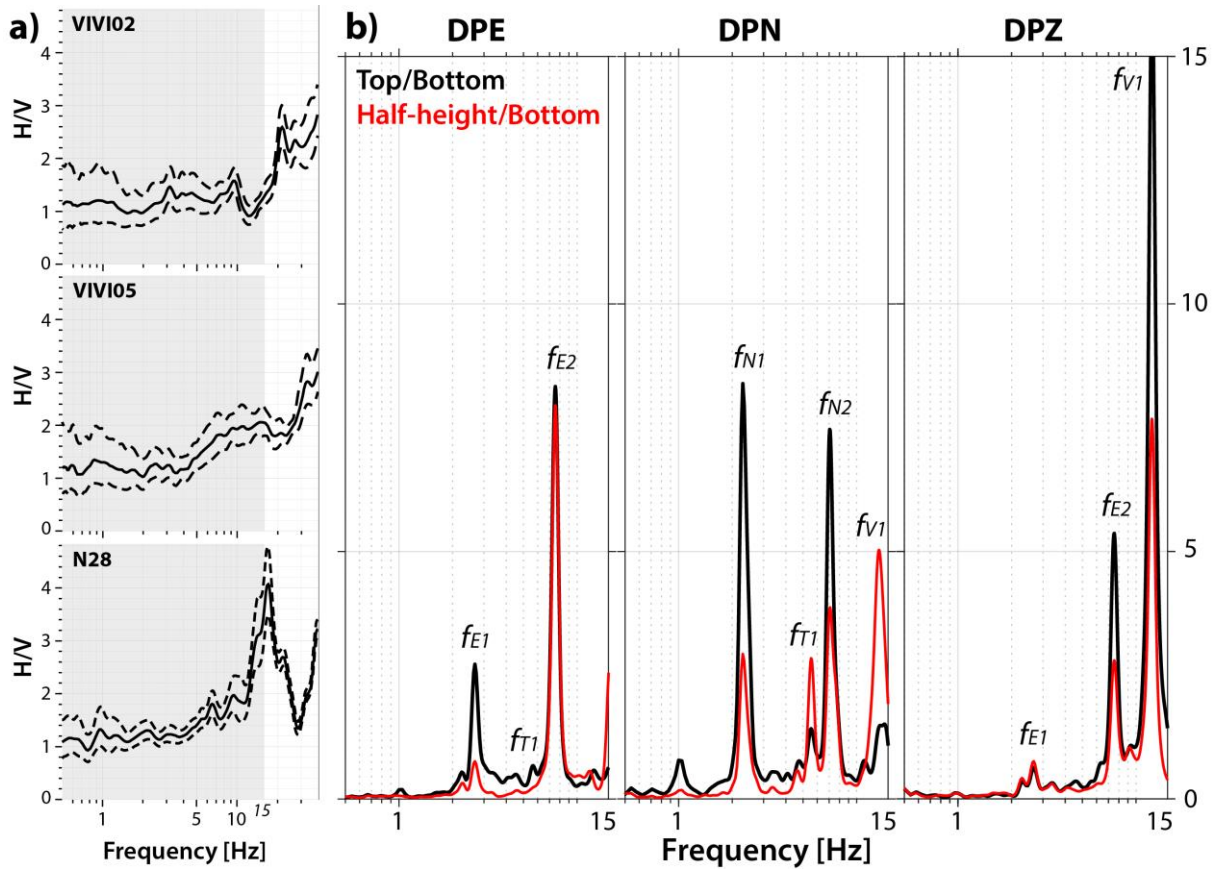

Fig.5 a) H/V measurements coming from two places of the episcopal quarter north of the Gate Tower (VIVI02/VIVI05) and from the node at the bottom of the Tower (N28); b) Spectral ratios performed on 2h of ambient noise (Nov. 20, 2019) between N17 and N28 (in black) and between N20 and N28 (in red). Comparison of those spectra evidences dissimilar patterns of solicitation of the two main parts of the Tower, particularly regarding the first torsion mode (f_{T1}).

On January 10 and 16, 2020, the nodes recorded the two first quarry blasts triggered in the Le Teil quarry two months after the November 11, 2019 mainshock. Due to the proximity of the GTV to the open pit, the monument was not only sensitive to the ground motions following the explosions but also to the acoustic blasts (Fig.6b). Figure 8 compares the frequency content of these two types of transient signals for the two quarry blasts. While the seismic signals resulting from the explosions led to a similar excitation of the building modes to that recorded during the seismic events – i.e. almost exclusively the first and second bending modes were excited – the acoustic signals (blasts) were associated with an excitation mainly in the N-S component. Located N350° with respect to the GTV, the explosions generated, therefore, a preferential deformation on the northern façade of the building. The striking presence of a large amplitude

peak at f_{N1} in the E-W component is likely due to the complexity of the bending mode shape of f_{N1} and f_{E1} in the upper octagonal part of the GTV.

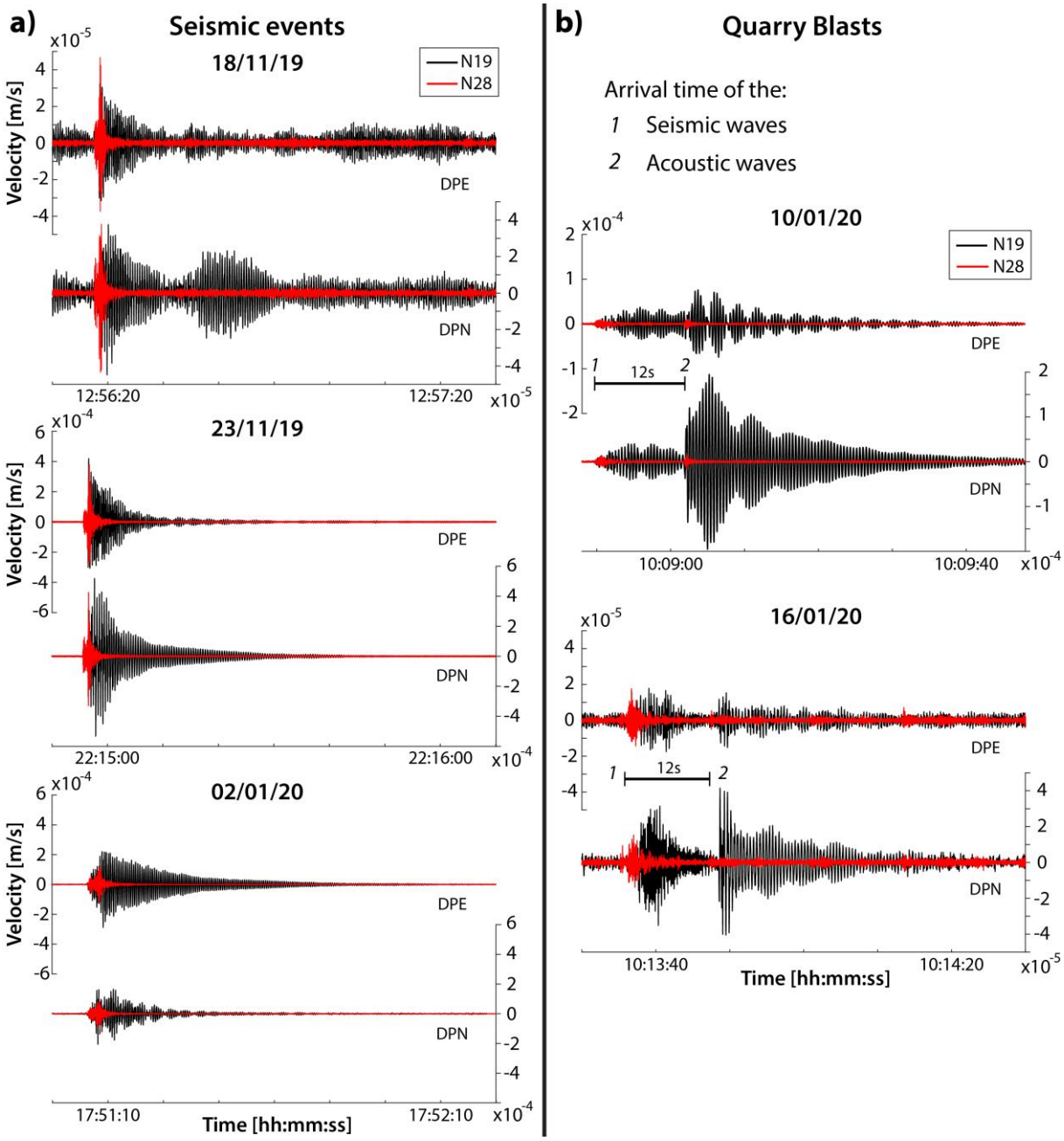

Fig.6 Velocities recorded in the two horizontal components during the three investigated seismic events (a) and the two quarry blasts (b) at the foot (in red) and the top (in black) of the structure. Regarding the quarry blasts, the GTV was also sensitive to the acoustic waves resulting from the explosion and following the traditional seismic signal.

Due to its proximity with the quarry (~5 km), the GTV was more sensitive to the blasts. The maximum amplitudes corresponding to the bending modes at f_{N1} and f_{E1} at the top of the Tower is indeed close to the amplitude of these two modes during the magnitude 2.2 and 2.7 seismic events (Fig.6). Finally, the amplitudes of the first bending mode in the two horizontal components are more than 8 times higher during the blast on January 10 than during the blast on January 16 and the torsion mode is excited markedly. This result might seem surprising given the similar characteristic and location (Tab.1-Fig.S2) of both quarry blasts. On January 10, 2020, the quarry blast was nonetheless triggered at the top of the quarry, unlike the one on January 16. That suggests a damped acoustic blast resulting from the second explosion (e.g. due to topography) until the town of Viviers. Interestingly, the dynamic behaviour analysis of the GTV demonstrates the differential response that may have such old masonry buildings to signals generated by similar (shallow and close) explosive sources.

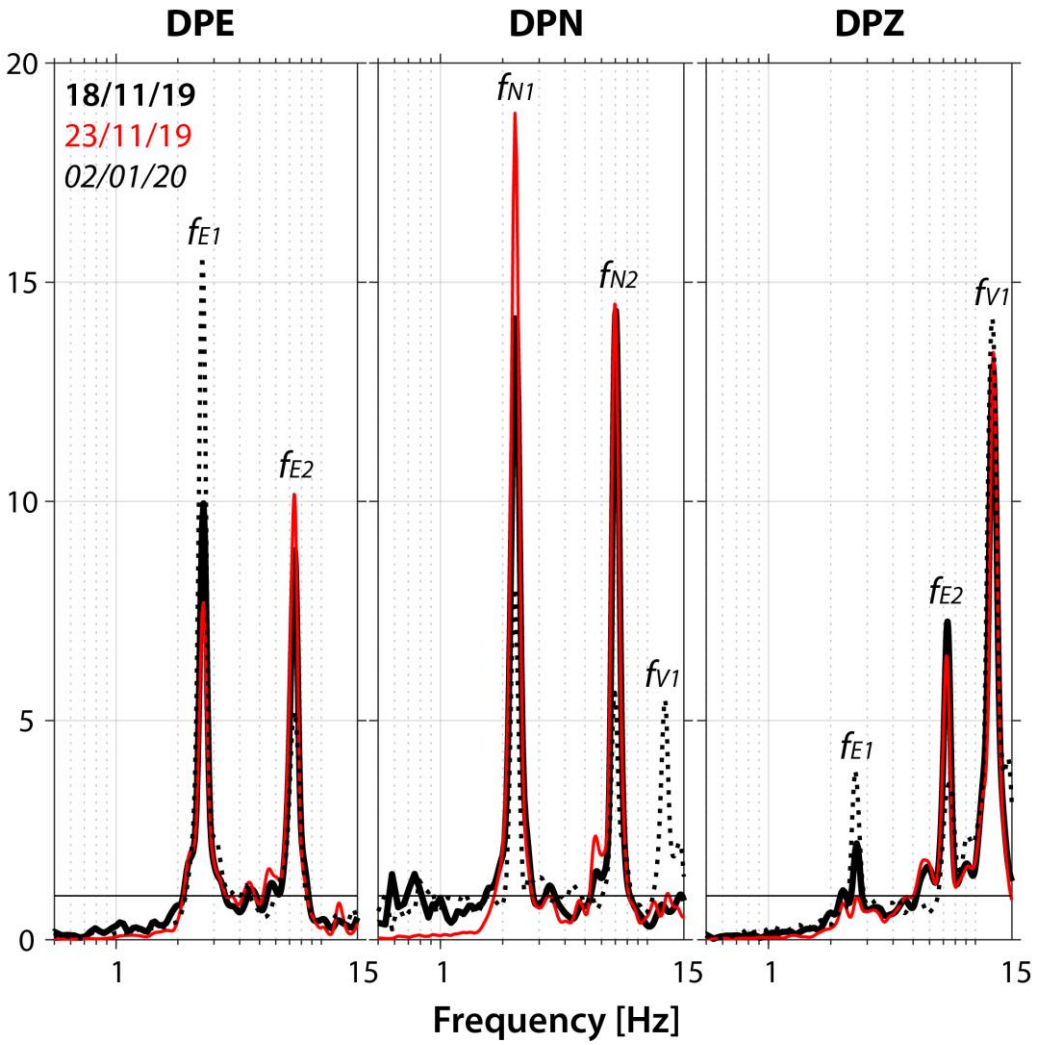

Fig.7 Spectral ratios performed between the top (N17) and the bottom (N28) of the GTV during the three seismic events (black, red and dotted).

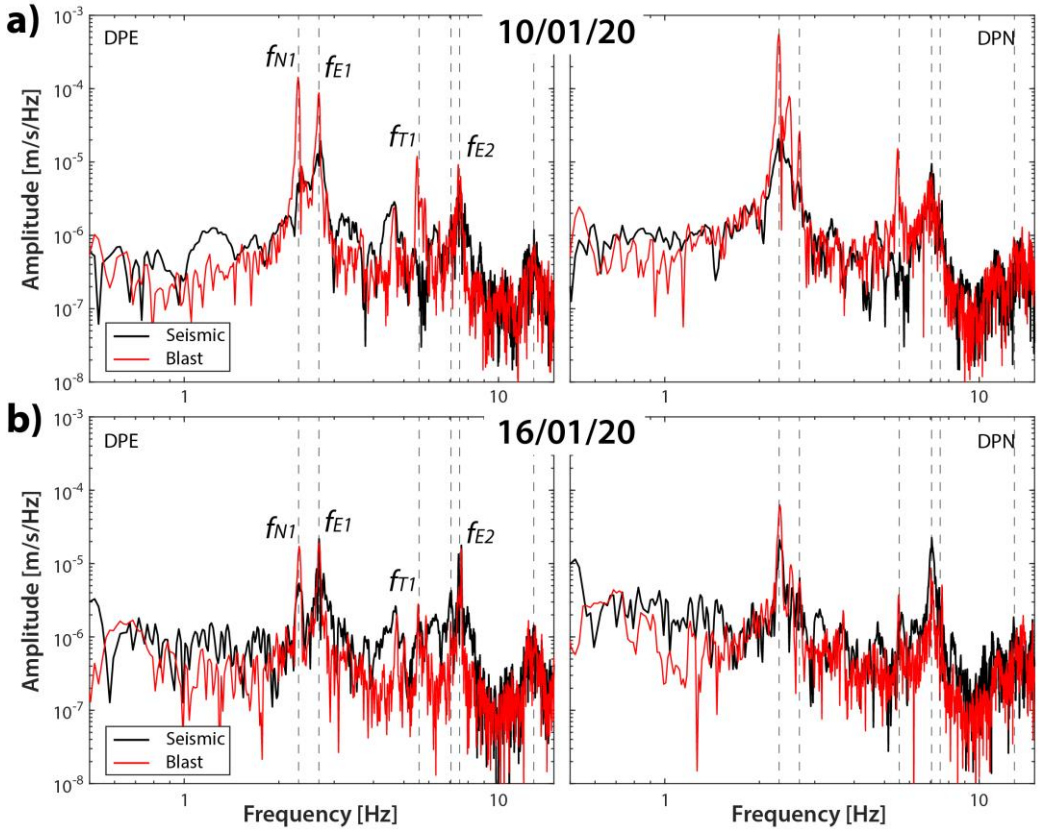

Fig.8 Comparison of the Tower's responses to the seismic (black) and acoustic (red) signals generated by the January 10 (a) and January 16 (b) quarry blasts at the top of the GTV (N19) in the two horizontal components. The acoustic "blast" on (a) January 10, 2020 induces a strong excitation of the first vibrations modes of the building (f_{N1}, f_{E1}, f_{T1}).

3.2. Influence of environmental factors

As already highlighted by previous works on reinforced concrete buildings (e.g., Clinton et al., 2006; Herak and Herak, 2010; Mikael et al., 2013; Guéguen et al., 2016; Wu et al., 2017), and masonry constructions (e.g., Cantieni, 2015; Ubertini et al., 2017; Azzara et al., 2018; Saisi et al., 2018) the wandering of structural parameters depends strongly on external factors and particularly on environmental conditions. Assessing the role of these environmental factors in the short and long-term variability of the modal parameters is thus a key issue towards a suitable condition assessment, especially for complex historic structures. Recent works (Mikael et al., 2013; Guéguen et al., 2016) have demonstrated the relevancy of the Random Decrement Technique, first proposed by Cole (1973), in reinforced concrete buildings to follow very slight variations of the resonant frequencies and damping ratios. In this study, we apply and check the relevance of the RDT to a more heterogeneous medium.

Continuous data were first converted into one-hour files. No overlap was set up between these time windows. The RDT was implemented by filtering around the resonant frequencies presented in Section 3.1. We adapted the band-pass filter to each target frequency mode (± 10% for f_{N1}, f_{E1}, ± 8% for f_{T1}, f_{V1} and ± 5% for f_{N2}, f_{E2}). We compared then the wandering of the natural frequencies and damping ratios with the variation of several weather parameters (temperature, humidity, wind speed and rainfalls) provided by a weather station (see Data and Resources Section) located less than 2 km northwest of the GTV (Fig.1).

Table 2 presents the mean values of the modal frequencies (μf) and associated damping coefficients ($\mu\xi$) computed over the monitoring period. It also contains the standard deviation (σ) and coefficient of variation for both modal parameters (COV). Note that the mean value of the coefficients of variation of the natural frequencies is less than 1%, i.e. more than thirty times smaller than the mean of the coefficients of variation of the damping coefficients. This simultaneously illustrates the intrinsic variability of damping values under weak motion (Brossault et al., 2018) and the greater calculation uncertainties related to the complex nature of damping mechanisms (Kareem and Gurley, 1996; Magalhães et al., 2010; Koruk and Sanliturk, 2011; Mikael et al., 2013). The first five vibration modes are characterized by very low damping coefficients (Tab.2), inferior to 1% (from f_{N1} to f_{E2}). Only the vertical mode (f_{V1}) is presenting values around 1.5-2%. Such low values of damping are rather unusual for tall masonry structures (Gentile and Saisi, 2007; Cantieni, 2015; Lacanna et al., 2016; Azzara et al., 2018).

We observe (Tab.2 and Fig. 9) a strong dependence of the frequency and damping values to weather conditions and according to different timescales: monthly-seasonal variations, day-night cycles as well as short events of a few hours. The GTV demonstrates, first, a strong sensitivity to temperature variations. A clear positive correlation is observed between the temperature and the frequency variations. Temperature variations of almost 125% (-2.2 to 18.6°C) compared to the mean value result thus in frequency variations around 3% for the first bending mode in the N-S component (Fig.9a-c). Although no global conclusions can be drawn on the nature of this correlation since the structural behaviour related to temperature variations may vary greatly from one building to another (Mikael et al., 2013), the current trend has also been reported for other historic masonry buildings (Casciati et al., 2014; Ubertini et al., 2017; Azzara et al., 2018). Thermal dilatation due to the increase in temperature leads to an apparent stiffening of the GTV by the closure of pores and cracks. This phenomenon is illustrated in Figure 10a by a phase shift in time between temperature and frequency variations due to thermal inertia. The positive correlation deviates from the linearity over 13-14°C (black arrow in

Fig.10b) and natural frequencies tend to increase more significantly above this threshold. This result coincides with observations reported in Cabboi et al. (2017). Our results suggest the decisive role of structural elements and pre-existing weaknesses of the masonry in the expansion-contraction cycles related to daily variations of temperature.

	Mode	f_{N1}	f_{E1}	f_{T1}	f_{N2}	f_{E2}	f_{V1}
DPE	**μ*f* [Hz]**		2.6807	5.5871		7.5180	
	σ*f* [Hz]		0.0217	0.0606		0.0489	
	COVf		0.0081	0.0108		0.0065	
	μξ [%]		0.4986	0.6899		0.2993	
	σξ [%]		0.0921	0.1835		0.1428	
	COVξ		0.1847	0.2660		0.4771	
DPN	**μ*f* [Hz]**	2.3109		5.5682	7.0590		12.952
	σ*f* [Hz]	0.0237		0.0702	0.0527		0.1270
	COVf	0.0103		0.0126	0.0075		0.0098
	μξ [%]	0.5630		0.8102	0.3583		1.4488
	σξ [%]	0.1022		0.3746	0.0665		0.5621
	COVξ	0.1815		0.4624	0.1856		0.3880
DPZ	**μf [Hz]**		2.6806			7.5149	12.186
	σf [Hz]		0.0219			0.0459	0.0935
	COVf		0.0082			0.0061	0.0077
	μξ [%]		0.6244			0.3304	1.9218
	σξ [%]		0.2243			0.1509	0.9765
	COVξ		0.3592			0.4567	0.5081
Temp.	**μ [°C]**	7.9550					
	σ [°C]	4.1962					
	COV	0.5275					
Wind	**μ [kph]**	5.4023					
	σ [kph]	5.0088					
	COV	0.9272					

Table 2 Table summarizing the mean frequency and damping values (μf, μξ), their associated uncertainties (σf, σξ) and the coefficient of variation (COV) for each mode of vibration in the three components computed with the RDT. Mean value (μ), standard deviation (σ) and coefficient of variation (COV) of the temperature and wind speed datasets are also indicated.

Located in the middle Rhône valley, the GTV is frequently exposed to moderate to strong wind events. The effect of wind may represent an important source of loading for tall buildings (Mendis et al., 2007) and may alter noticeably their response (Li et al., 2010; Wu et al., 2017; Azzara et al., 2019). The time histories of the GTV do not support a correlation (R^2<0.05)

between frequency variations and wind speed (Fig.9a-e, Fig.S3), contrary to the findings from Li et al. (2010) and Wu et al. (2017) for reinforced concrete buildings. We can observe, nonetheless, significant frequency drops corresponding to a softening of the structure during the windiest periods (wind velocities >15km/h).

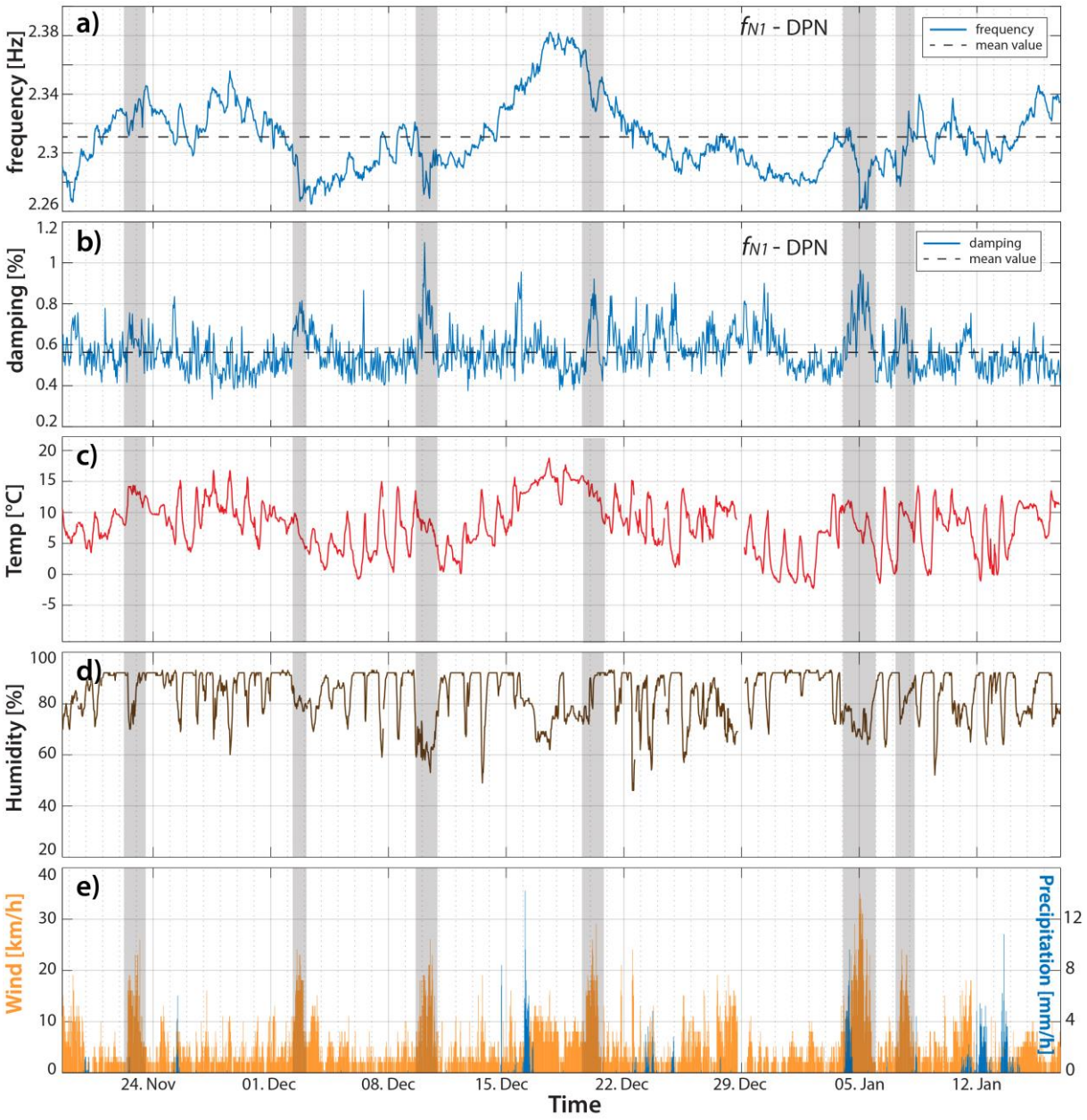

Fig.9 Frequency and damping fluctuations (a and b) of the first bending mode in the N-S component (f_{N1}) compared to the variations of weather parameters: temperature (c), moisture (d), wind and precipitation (e). Shaded areas indicate the windiest periods.

Notwithstanding the large uncertainties in the estimation of the absolute coefficients of damping – illustrated by the large scatter among the data –, the variations of the damping ratios evidence a positive correlation with the wind velocity. Figure 9b and 9e show the coincidence of the windiest periods, for instance on December 10, December 20, 2019 and January 05, 2020, and the damping maxima. More generally the wind dataset exhibits a satisfactory coefficient of determination (R^2~0.10-0.15) when plotted with damping values (Fig.10c). Despite the reduced sample size of windy hours, the covariance tends to increase as wind speed increases. This observation is in agreement with conclusions from Wu et al. (2017) and Azzara et al. (2017). In the case of strong wind velocities, wind speed turns out to be the dominant contributor in terms of ambient excitation, driving thus the Tower's response. The wind has, nevertheless, a lesser influence on the torsion mode (Fig.10c). In addition, damping variations seem to correlate simultaneously with the humidity level (Fig.9b-d). Although this finding is not surprising due to the strong impact of wind velocities on the degree of moisture, it raises the strong interdependency of many meteorological factors.

In addition, we were not able to see any clear correlation between the temperature and the damping variations (Fig.S3). The effect of the stiffening observed on frequency during the hottest periods has no impact on damping or is completely blurred by the wind gusts. Finally, rainfalls do not show any appreciable effect on frequency and damping variations. However, a correlation cannot be ruled out due to the scanty amount of precipitation recorded during the monitoring period.

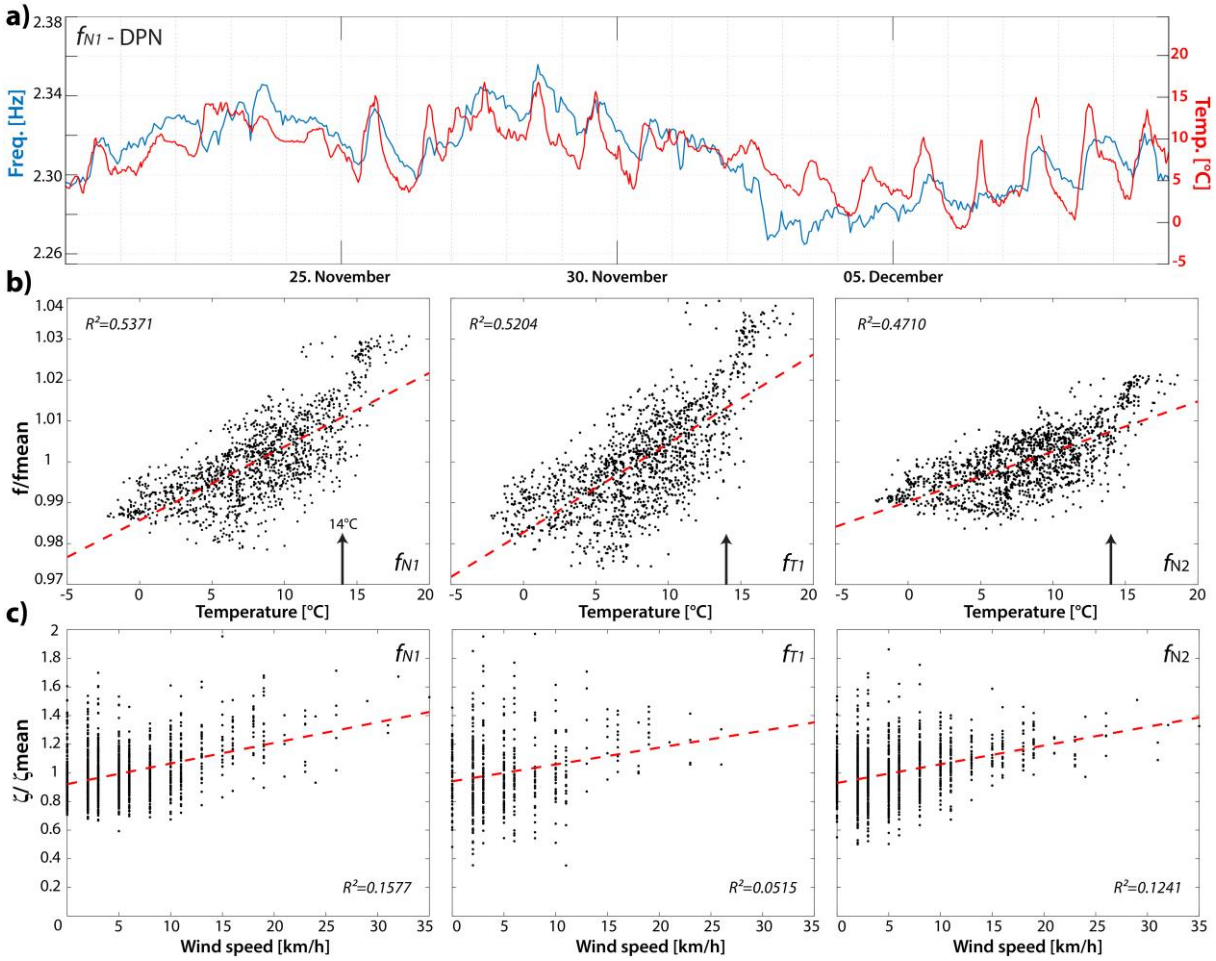

Fig.10 a) Fluctuations of the frequency of the first bending mode in the N-S component (in blue) and the temperature values (in red) measured between Nov. 20 and Dec. 10, 2019; b) Correlation between temperature and normalized frequency for the first bending mode, the torsion mode and the second bending mode (left to right) in the N-S component; c) Correlation between wind speed and normalized damping for the same modes as b). Despite the large scatter of point clouds, the data seem to follow linear relations. Plots are based on the recordings of N19.

Summarizing the main observations:

- The rise of temperature induces an apparent stiffening of the building. Unlike reinforced concrete buildings, historic masonry structures are highly heterogeneous media. Pores and cracks that characterize the eleventh-century construction make it particularly sensitive to thermal effects.
- Strong wind gusts that periodically affect the middle Rhône valley represent a major source of atmospheric loading, influencing therefore strongly the damping variations. However, the wide dispersion of the results displayed in Figure 10c highlights both the

uncertainties related to the estimation of the damping (Kareem and Gurley, 1996) and the complex nature of its wandering in structures (Mikael et al., 2013; Guéguen et al., 2016). This modal parameter seems to be "loading dependent" and is therefore mainly driven in our case by the wind forcing.

- Accordingly, our results support rather uncorrelated variations of the frequency and damping values. The results presented in this section demonstrate that both structural parameters are conditioned mainly by distinct external factors. Whereas frequency appears to be exclusively temperature dependant, the damping ratio seems to be influenced particularly by the wind velocity. In other words, notwithstanding the wide spectrum of environmental factors that may have an impact on the dynamic response of buildings, temperature controls predominantly the stiffness of the building, while wind blow has a higher impact on damping fluctuations. In both cases, weather conditions lead to significant variations of modal parameters regarding the first vibration modes (f~3% and ξ~60%).

3.3. Nonlinear elasticity

Several works at different scales have yet observed significant alterations of the elastic properties of materials and structures under moderate loadings and not associated though to apparent damage (Johnson and Sutin, 2005; Brossault et al., 2018). The causes behind this phenomenon remain unclear but seem to be related to the rearrangement of the internal components of the material and/or structure, entailing variations in their physical properties (Guyer and Johnson, 2009; Brossault et al., 2018). Highly heterogeneous and fractured media, the historic masonry buildings might be particularly sensitive to nonlinearity. The variations of modal parameters are then studied as a function of the deformation of the GTV, computed as the structural drift between the top and the bottom (D).

We calculated the mean drift for the 1,426 one-hour time windows of ambient vibrations and compared it with the associated frequencies and damping values (Fig.11). We, first, filtered around the resonant frequencies in order to assess the deformation related to each vibration mode of the Tower. Then, the displacement was obtained by integrating the velocities following the recommendation of Boore (2005). The drift value for each 1h-window was then calculated as the difference of the root mean square (RMS) displacements at the top (N19) and at the base (N28) of the structure divided by its height (37m). Moreover, the dataset was divided based on temperature intervals (ΔT=2°C) to reduce as much as possible the influence of this weather parameter detailed in 3.2.

Figure 11a-b displays frequency and damping variations of the first bending mode in the N-S component (f_{N1}), as a function of drift, for the temperature interval 8-10°C. Frequency and damping coefficients were normalized by the first 10% of the dataset corresponding to the lowest drift values, i.e. representing the frequency and damping values of the linear domain (f_0 and ξ_0 respectively). Three transient events fall within the temperature interval: the November 23, 2019 aftershock as well as the two quarry blasts. According to Guéguen et al. (2016) who demonstrated the applicability of the RDT on short time windows to track sudden variations of modal parameters associated with ground shakings, we calculated the frequency and damping coefficients on 40sec and 15min windows, respectively (stars and diamonds in Fig.11a-b).

In a similar manner to previous studies on reinforced concrete structures (Guéguen et al., 2016) and modern brick masonry buildings (Michel et al., 2011), the results highlight a clear nonlinear behaviour independently from temperature fluctuations. Regarding f_{N1}, we note a first trend (Fig.11a) with stable frequency and damping values (<1% fluctuations for frequency and <20% for damping). Over a certain threshold D_0 (~10^{-8}), the stiffness of the structure appears to decrease significantly (2-3%) and the damping increases (40-80%).

Regarding the effect of transient events recorded during this specific temperature interval, the results fit well with the global trend discussed above. The drift values associated with the one-hour windows including the considered ground shakings (coloured dots on Fig.11a-b) do not attest properly from the deformation following the events. The magnitude and duration of the events are indeed too small to induce noticeable changes on one-hour windows. More surprising, drift values calculated on 40sec (*f*-variations – stars on Fig.11a) and 15min (ξ-variations – diamonds on Fig.11b) windows do not exceed much the range of values from ambient vibration recordings.

Drift results from the GTV are in agreement with the observations of Michel et al. (2011) and Guéguen et al. (2016) who identified, within the elastic domain, a threshold in the dynamic behaviour of masonry structures beyond which internal micro-cracks start to open progressively, modifying the overall response of the structure to dynamic strains. In our case, the onset of the nonlinear elastic response (D_0) appears at much lower drift values (Fig.11a-b) than documented by the previous authors for reinforced concrete and modern brick masonry structures. This finding is not surprising owing to the high heterogeneity level of the building that is indeed controlling the nonlinear response (Astorga et al., 2018; Brossault et al., 2018).

As noted in Section 3.2, the damping values are more scattered than natural frequencies and part of this dispersion cannot be explained by the sole calculation uncertainties (Guéguen et al., 2016). Figure 11a-b shows the linear fits of the frequency ($f(D)=a*\log(D)+c$) and damping

variations ($\xi(D)=b*\log(D)+d$) and their associated slope values under and over D_0 (a_1-b_1 and a_2-b_2 respectively). The slope values over D_0 are more than ten times higher for damping coefficient (b_2 in Fig.11b) than for natural frequencies (a_2 in Fig.11a) that highlights the stronger sensitivity of the damping to the level of strain and loading. As demonstrated on Plexiglas and limestone beams by Brossault et al. (2018), the level of damping variation under weak loading is directly correlated to the heterogeneity of the material according to the fluctuation-dissipation theorem. In our case, the sharp rupture of the slope over D_0 confirms, therefore, the highly heterogeneous nature of the Tower and suggests a significant role of those heterogeneities in the damping values under low levels of strain.

Figure 11c presents the values of the slope b_2 of the linear fit ($\xi(D)=0.8585*\log(D)+6.7570$) applied to the damping values over D_0 for each ΔT. b_2 values increase gradually with the increase of the temperature until reaching a maximum at around 13-14°C.

Brossault et al. (2018) have shown the relation between the inner heterogeneities of beam-like structures and the slope of the damping values variation under weak loading. Applied to the GTV, this reflects the variation of the inner structure of the tower with temperature (e.g., the number of opened cracks), which influences the wandering of the damping values observed under weak loading. This wandering reflects the activation of the number of cracks with the amplitude of the loading (in our case the wind speed). At a certain value of temperature (13-14°C), the slope of the linear damping – and loading – relationship is not changing anymore, explained by the stable inner structure above this temperature and the constant number of activated cracks. Thus, the apparent stiffening of the GTV with the increase of temperature (Fig. 10b) below 14°C would be due to the closure of the structural defaults (Cabboi et al., 2017), associated with the increase of b_2. The reduction of the b_2 slope above 14°C coincides with the faster increase of natural frequencies mentioned earlier (black arrows in Fig.10b). The underlying processes that explain this observation are not yet identified but the role of the structural heterogeneities (e.g., cracks) is assumed, in relation to the expansion-contraction cycles related to thermal effects and the influence of the multiphasic structure of the masonry (particularly the mortar interface). Further research is needed to assess a possible correlation and address the complex contribution of the factors driving the damping variation.

However, we support that the very strong structural heterogeneity, which characterizes historic masonry buildings, constitutes one of the main contributors of this nonlinearity (Guyer and Johnson, 2009; Brossault et al., 2018) and might be responsible for the very low threshold D_0 observed herein. The complex building fabric of the Tower, composed of limestone blocks of different sizes connected with a heterogeneously distributed soft mortar echoes well, although

at a different scale, with the “bond system” described by Johnson and Sutin (2005). The block-mortar interface as well as the numerous pre-existing fractures and vulnerabilities that characterize old masonries may act as the “bond system”, increasing the energy dissipation through friction and dilatation.

This discussion raises the further issue: is an ambient vibration-based instrumentation of a historic masonry building sufficient to monitor slight and progressive degradations of its structural state? The results confirm the interest in tracking and quantifying the nonlinear behaviour of the damping coefficient, and this despite the difficulties to estimate it precisely in complex systems like buildings. More sensitive to the level and distribution of heterogeneities, this parameter might become a relevant proxy for SHM and a relevant warner of damage, at an early stage (Modena et al., 1999; Guéguen et al., 2016; Brossault et al., 2018).

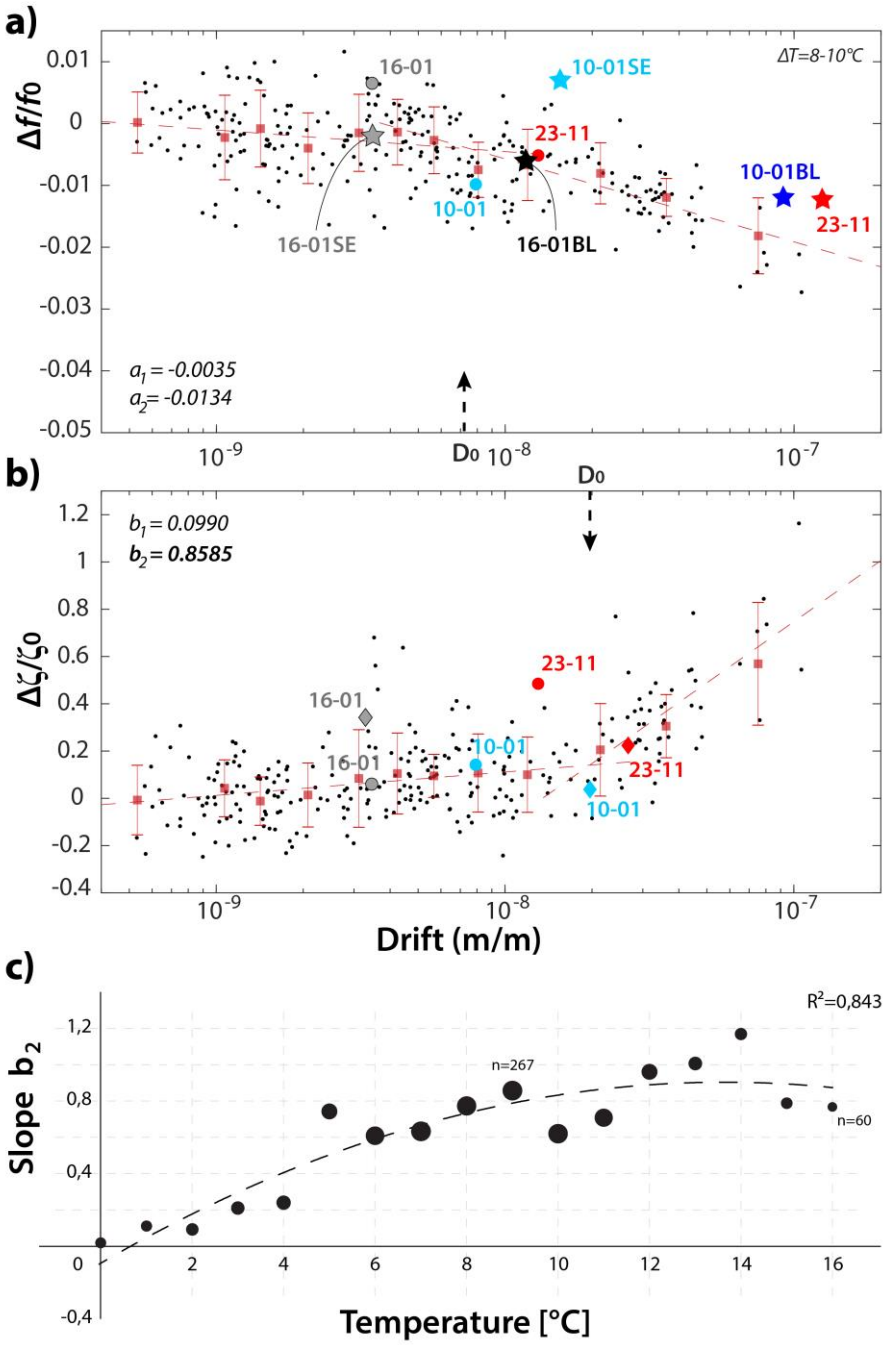

Fig.11 Variation of the normalized frequency (a) and the associated damping (b) of the first bending mode as a function of the drift of the structure for the temperature interval 8-10°C. Error bars indicate the average (red square) and standard deviation values (vertical red lines) computed by bins of 23 consecutive values. Large coloured dots correspond to the one-hour windows including the Nov. 23 aftershock and the two quarry blasts. Coloured stars and diamonds correspond to values calculated respectively on 40s and 15min windows containing those transient signals. On 40s windows, we distinguished between the GTV's response to the seismic (SE) and acoustic (BL) signals of the quarry blasts; c) Evolution of the damping variations according to thermal conditions. Dots are scattered by the size of the sample.

4. Conclusions

As Ahmad and Ali (2017, p. 4) noticed, “the behaviour of masonry material is dramatically different from the counterpart concrete and steel material due to high non-homogeneity and composite nature of masonry components.” This strong heterogeneity “makes the masonry behaviour difficult to predict.” The concern is thus even more acute for cultural heritage buildings. Conducting ambient vibration measurements has proved to be a valuable tool to deepen the knowledge on their global dynamic behaviour, develop more realistic numerical models (Sivori et al., 2020), improve the seismic response predictions and support the decision-making (Ercan, 2018; Reuland et al., 2019) while limiting our imprint on those vulnerable structures. The Mw 4.9 Le Teil earthquake, i.e. the strongest seismic sequence in mainland France since the 1967 Arette and 1996 Epagny earthquakes, stresses the necessity to foster research even in areas affected by a low to a moderate seismic hazard. The instrumental survey implemented in the GTV immediately after the mainshock contributes to improving our understanding of a complex and emblematic monument of the middle Rhône valley. More generally, our work acts as a baseline and demonstrates the relevance of several methods for the analysis of the elastic response of ancient masonry buildings to both quasi-static (atmospheric) and dynamic (aftershocks and blasts) loadings.

In a first step, the OMA allows the identification of the first six structural modes of the GTV. The moderate transient signals recorded during its monitoring confirm the empirical structural model obtained from the ambient vibration data but reveal a different response of the monument to very near ground shakings. An interesting additional finding: historic masonry structures may show a remarkably strong sensitivity to acoustic blasts generated by nearby triggered explosions.

Secondly, the application of the RDT to the GTV monitoring demonstrates the robustness of this signal processing method to track slight variations of the modal parameters in function of time and the strong influence of environmental factors on their wandering. Our results support a major contribution of temperature fluctuations on the apparent stiffness of the structure while damping variations appear more strongly influenced by the local wind gusts, the primary source of atmospheric loading. The effects of weather conditions are of the same order of magnitude or even stronger than those of the aftershocks and quarry blasts.

Last but not least, we highlight the non-linear elastic response of the unreinforced masonry constructions under particularly low levels of strain and stress the major role of the heterogeneities and pre-existing fragilities in dissipating the energy. While previous studies

have yet demonstrated the interest in tracking frequency shift for damage identification (Michel and Gueguen, 2010; Cavalagli et al., 2017), our results show the greater sensitivity of the damping ratio to the level of heterogeneity of the structure and the complex interactions existing between the mobilization of those structural weaknesses and the environmental conditions. While further research is required to remove the influence of environmental effects on the fluctuation of the damping coefficient, the present work argues for considering it as a promising tool for SHM and conservation efforts dedicated to the built heritage.

Data and Resources

Information on the historical seismicity and its impact on the GTV is available on the database of historical earthquakes SisFrance (https://www.sisfrance.net/; last accessed January 02, 2022).

The Résif-EPOS (French permanent seismological network) data centre gathers the whole regional seismological dataset into a homogeneous archive and provides access to the data through FDSN web services (Péquegnat et al., 2021). The seismological data and metadata from this survey are therefore freely available through the Résif-EPOS portal (https://ws.resif.fr/ - last accessed January 02, 2022; network 3C - http://dx.doi.org/10.15778/RESIF.3C2019).

Weather parameters were downloaded from an open-access weather station using https://www.infoclimat.fr/observations-meteo/archives/15/septembre/2019/viviers/000U8.html#! (last accessed January 02, 2022 – StatIC network).

The supplemental material for this article includes the spectral densities of the aftershocks (Nov 18, 2019, Nov 23, 2019 and Jan 02, 2020) and the quarry blasts (Jan 10 and Jan 16, 2020) computed at two free-field stations (VIVI and CLAU - network 3C). Inconclusive correlations between weather and structural parameters are included also.

Acknowledgments

We would first express our kindest thanks to Martine Moron, technical expert at the “Bâtiments de France”, who facilitated greatly the instrumental survey by giving us the access to the Tower. We acknowledge Christophe Voisin and the SIG (Geophysical instrumentation service) team for their support during the field campaign and for their technical assistance regarding the Fairfield ZLand nodes. We are also grateful to Yves Esquieu who gave us the access to architectural and archaeological resources related to the Gate Tower and shared with us its

expertise on the historic city centre of Viviers. Finally, we would like to show our gratitude to the two “anonymous” reviewers and the editor whose suggestions helped improve and clarify this manuscript.

This work has been realised in the framework of the IDEX CDP Risk@Univ. Grenoble Alpes as part of the program “Investissements d’Avenir” overseen by the French National Research Agency (ANR-15-IDEX-02). The project has received, as well, financial support from the Auvergne Rhône-Alpes region through the AURA PAI project and field experiments were supported by funding from Action Transversale Sismicité (ATS) of RESIF. RESIF is a national Research Infrastructure recognized as such by the French Ministry of higher education and research. It is additionally supported by a public grant overseen by the French national research agency (ANR) as part of the “Investissements d’Avenir” program (reference: ANR-11-EQPX-0040) and the French Ministry of ecology, sustainable development and energy.

References

Ahmad, N., and Q. Ali, 2017, Displacement-based seismic assessment of masonry buildings for global and local failure mechanisms, Cogent Engineering, 4, no. 1, 1414576, doi: 10.1080/23311916.2017.1414576.

Astorga, A., P. Guéguen, and T. Kashima, 2018, Nonlinear Elasticity Observed in Buildings during a Long Sequence of Earthquakes, Bulletin of the Seismological Society of America, 108, no. 3A, 1185–1198, doi: 10.1785/0120170289.

Astorga, A. L., P. Guéguen, J. Rivière, T. Kashima, and P. A. Johnson, 2019, Recovery of the resonance frequency of buildings following strong seismic deformation as a proxy for structural health, Structural Health Monitoring, 18, nos. 5–6, 1966–1981, doi: 10.1177/1475921718820770.

Azzara, R., A. De Falco, M. Girardi, and D. Pellegrini, 2017, Ambient vibration recording on the Maddalena Bridge in Borgo a Mozzano (Italy): data analysis., Annals of Geophysics, 60, no. 4, S0441, doi: 10.4401/ag-7159.

Azzara, R. M., G. De Roeck, M. Girardi, C. Padovani, D. Pellegrini, and E. Reynders, 2018, The influence of environmental parameters on the dynamic behaviour of the San Frediano bell tower in Lucca, Eng. Struct., 156, 175–187, doi: https://doi.org/10.1016/j.engstruct.2017.10.045.

Azzara, R. M., M. Girardi, V. Iafolla, D. M. Lucchesi, C. Padovani, and D. Pellegrini, 2019, Ambient Vibrations of Age-old Masonry Towers: Results of Long-term Dynamic Monitoring in the Historic Centre of Lucca, International Journal of Architectural Heritage, 18, doi: 10.1080/15583058.2019.1695155.

Barsocchi, P., G. Bartoli, M. Betti, M. Girardi, S. Mammolito, D. Pellegrini, and G. Zini, 2020, Wireless Sensor Networks for Continuous Structural Health Monitoring of Historic Masonry Towers, International Journal of Architectural Heritage, 15, no. 1, 22–44, doi: 10.1080/15583058.2020.1719229.

Boore, D. M., 2005, On Pads and Filters: Processing Strong-Motion Data, Bulletin of the Seismological Society of America, 95, no. 2, 745–750, doi: 10.1785/0120040160.

Brincker, R., L. Zhang, and P. Andersen, 2001, Modal identification of output-only systems using frequency domain decomposition, Smart Mater. Struct., 10, no. 3, 441–445, doi: 10.1088/0964-1726/10/3/303.

Brossault, M.-A., P. Roux, and P. Guéguen, 2018, The fluctuation–dissipation theorem used as a proxy for damping variations in real engineering structures, Engineering Structures, 167, 65–73, doi: 10.1016/j.engstruct.2018.04.012.

Cabboi, A., C. Gentile, and A. Saisi, 2017, From continuous vibration monitoring to FEM-based damage assessment: Application on a stone-masonry tower, Construction and Building Materials, 156, 252–265, doi: 10.1016/j.conbuildmat.2017.08.160.

Cantieni, R., 2015, One-Year Monitoring of a Historic Bell Tower, Key Engineering Materials, 628, 73–78, doi: 10.4028/www.scientific.net/KEM.628.73.

Casciati, S., A. Tento, A. Marcellini, and R. Daminelli, 2014, Long run ambient noise recording for a masonry medieval tower, Smart Structures and Systems, 14, no. 3, 367–376, doi: 10.12989/SSS.2014.14.3.367.

Causse, M., C. Cornou, E. Maufroy, J.-R. Grasso, L. Baillet, and E. El Haber, 2021, Exceptional ground motion during the shallow Mw 4.9 2019 Le Teil earthquake, France, Commun Earth Environ, 2, no. 1, 14, doi: 10.1038/s43247-020-00089-0.

Cavalagli, N., G. Comanducci, C. Gentile, M. Guidobaldi, A. Saisi, and F. Ubertini, 2017, Detecting earthquake-induced damage in historic masonry towers using continuously monitored dynamic response-only data, Procedia Engineering, 199, 3416–3421, doi: 10.1016/j.proeng.2017.09.581.

Ceravolo, R., G. Pistone, L. Z. Fragonara, S. Massetto, and G. Abbiati, 2016, Vibration-Based Monitoring and Diagnosis of Cultural Heritage: A Methodological Discussion in Three Examples, International Journal of Architectural Heritage, 10, no. 4, 375–395, doi: 10.1080/15583058.2013.850554.

Clemente, P., F. Saitta, G. Buffarini, and L. Platania, 2015, Stability and seismic analyses of leaning towers: the case of the minaret in Jam., Struct. Design Tall Spec. Build., 24, no. 1, 40–58, doi: 10.1002/tal.1153.

Clinton, J. F., S. C. Bradford, T. H. Heaton, and J. Favela, 2006, The Observed Wander of the Natural Frequencies in a Structure, Bulletin of the Seismological Society of America, 96, no. 1, 237–257, doi: 10.1785/0120050052.

Cole, H. A., 1973, On-line Failure Detection and Damping Measurement of Aerospace Structures by Random Decrement Signatures, CR-2205, NASA, Mountain View, California, 75 p.

Cornou, C. et al., 2020, Rapid response to the Mw 4.9 earthquake of November 11, 2019 in Le Teil, Lower Rhône Valley, France, Comptes Rendus Geosciences, doi: 10.31219/osf.io/3afs5.

Dogangun, A., R. Acar, H. Sezen, and R. Livaoglu, 2008, Investigation of dynamic response of masonry minaret structures, Bull Earthquake Eng, 6, no. 3, 505–517, doi: 10.1007/s10518-008-9066-5.

Elmi, S., R. Busnardo, B. Clavel, G. Camus, G. Kieffer, P. Bérard, and B. Michaëly, 1996, Carte Géologique de la France à 1/50 000 - Aubenas, BRGM, Orléans.

Ercan, E., 2018, Assessing the impact of retrofitting on structural safety in historical buildings via ambient vibration tests, Construction and Building Materials, 164, 337–349, doi: 10.1016/j.conbuildmat.2017.12.154.

Esquieu, Y., 1983, La cathédrale de Viviers et les bâtiments du cloître, XIIe-XIIIe siècles, Bulletin Monumental, 141, no. 2, 121–148, doi: 10.3406/bulmo.1983.6198.

Esquieu, Y. (ed.), 1988, Viviers, cité épiscopale: Études archéologiques, Alpara, Lyon.

Esquieu, Y., and R. Guild, 1992, Le campanile de la cathédrale de Viviers, in *Congrès archéologique de France, moyenne vallée du Rhône* Société française d'archéologie (Editor), Paris : Derache ; Caen : A. Hardel, Paris-Caen, 333–350.

Farrar, C. R., and K. Worden, 2007, An Introduction to Structural Health Monitoring, Phil. Trans R. Soc. A, 365, 303–315, doi: 10.1098/rsta.2006.1928.

Gentile, C., and A. Saisi, 2007, Ambient vibration testing of historic masonry towers for structural identification and damage assessment, Construction and Building Materials, 21, no. 6, 1311–1321, doi: 10.1016/j.conbuildmat.2006.01.007.

Guéguen, P., M.-A. Brossault, P. Roux, and J. C. Singaucho, 2020, Slow dynamics process observed in civil engineering structures to detect structural heterogeneities, Engineering Structures, 202, 109833, doi: 10.1016/j.engstruct.2019.109833.

Guéguen, P., P. Johnson, and P. Roux, 2016, Nonlinear dynamics induced in a structure by seismic and environmental loading, The Journal of the Acoustical Society of America, 140, no. 1, 582–590, doi: 10.1121/1.4958990.

Guyer, R. A., and P. A. Johnson, 2009, Nonlinear Mesoscopic Elasticity: The Complex Behaviour of Rocks, Soil, Concrete, John Wiley & Sons.

Herak, M., and D. Herak, 2010, Continuous monitoring of dynamic parameters of the DGFSM building (Zagreb, Croatia), Bull Earthquake Eng, 8, no. 3, 657–669, doi: 10.1007/s10518-009-9112-y.

Hinzen, K.-G., C. Fleischer, B. Schock-Werner, and G. Schweppe, 2012, Seismic Surveillance of Cologne Cathedral, Seismological Research Letters, 83, no. 1, 9–22, doi: 10.1785/gssrl.83.1.9.

Jaishi, B., W.-X. Ren, Z.-H. Zong, and P. N. Maskey, 2003, Dynamic and seismic performance of old multi-tiered temples in Nepal, Engineering Structures, 25, no. 14, 1827–1839, doi: 10.1016/j.engstruct.2003.08.006.

Johnson, P., and A. Sutin, 2005, Slow dynamics and anomalous nonlinear fast dynamics in diverse solids, The Journal of the Acoustical Society of America, 117, no. 1, 124–130, doi: 10.1121/1.1823351.

Kareem, A., and K. Gurley, 1996, Damping in structures: its evaluation and treatment of uncertainty, Journal of Wind Engineering and Industrial Aerodynamics, 59, nos. 2–3, 131–157, doi: 10.1016/0167-6105(96)00004-9.

Korswagen, P. A., M. Longo, and J. G. Rots, 2020, High-resolution monitoring of the initial development of cracks in experimental masonry shear walls and their reproduction in finite element models, Engineering Structures, 211, 110365, doi: 10.1016/j.engstruct.2020.110365.

Koruk, H., and K. Y. Sanliturk, 2011, Damping uncertainty due to noise and exponential windowing, Journal of Sound and Vibration, 330, no. 23, 5690–5706, doi: 10.1016/j.jsv.2011.07.006.

Lacanna, G., M. Ripepe, E. Marchetti, M. Coli, and C. A. Garzonio, 2016, Dynamic response of the Baptistery of San Giovanni in Florence, Italy, based on ambient vibration test, Journal of Cultural Heritage, 20, 632–640, doi: 10.1016/j.culher.2016.02.007.

Li, Hui, S. Li, J. Ou, and Hongwei Li, 2010, Modal identification of bridges under varying environmental conditions: Temperature and wind effects, Struct. Control Health Monit., 17, 495–512, doi: 10.1002/stc.319.

Magalhães, F., Á. Cunha, E. Caetano, and R. Brincker, 2010, Damping estimation using free decays and ambient vibration tests, Mechanical Systems and Signal Processing, 24, no. 5, 1274–1290, doi: 10.1016/j.ymssp.2009.02.011.

Mazzotti, S., H. Jomard, and F. Masson, 2020, Processes and deformation rates generating seismicity in metropolitan France and conterminous Western Europe, BSGF - Earth Sci. Bull., 191, 19, doi: 10.1051/bsgf/2020019.

Mendis, P., T. Ngo, N. Haritos, A. Hira, B. Samali, and J. Cheung, 2007, Wind Loading on Tall Buildings, EJSE, Special Issue: Loading on Structures, 41–54.

Micelli, F., and A. Cascardi, 2020, Structural assessment and seismic analysis of a 14th century masonry tower, Engineering Failure Analysis, 107, 104198, doi: 10.1016/j.engfailanal.2019.104198.

Michel, C., and P. Gueguen, 2010, Time-Frequency Analysis of Small Frequency Variations in Civil Engineering Structures Under Weak and Strong Motions Using a Reassignment Method, Structural Health Monitoring, 9, no. 2, 159–171, doi: 10.1177/1475921709352146.

Michel, C., P. Guéguen, S. El Arem, J. Mazars, and P. Kotronis, 2010, Full-scale dynamic response of an RC building under weak seismic motions using earthquake recordings, ambient vibrations and modelling, Earthquake Engng. Struct. Dyn., 39, no. 4, 419–441, doi: 10.1002/eqe.948.

Michel, C., B. Zapico, P. Lestuzzi, F. J. Molina, and F. Weber, 2011, Quantification of fundamental frequency drop for unreinforced masonry buildings from dynamic tests, Earthquake Engng. Struct. Dyn., 40, no. 11, 1283–1296, doi: 10.1002/eqe.1088.

Mikael, A., P. Gueguen, P. Bard, P. Roux, and M. Langlais, 2013, The Analysis of Long-Term Frequency and Damping Wandering in Buildings Using the Random Decrement Technique, Bulletin of the Seismological Society of America, 103, no. 1, 236–246, doi: 10.1785/0120120048.

Modena, C., D. Sonda, and D. Zonta, 1999, Damage Localization in Reinforced Concrete Structures by Using Damping Measurements, KEM, 167–168, 132–141, doi: 10.4028/www.scientific.net/KEM.167-168.132.

Nakamura, Y., 1989, A Method for Dynamic Characteristics Estimation of Subsurface Using Microtremor on the Ground Surface, Quarterly Report of Rtri, 30, no. 1, 25–33.

Naud, G., 2021, Les séismes de l'été 1873 dans le Tricastin. Déroulé et interpretations à l'époque puis de nos jours., SGA, 14, 29–38.

Pau, A., and F. Vestroni, 2008, Vibration analysis and dynamic characterization of the Colosseum, Struct. Control Health Monit., 15, no. 8, 1105–1121, doi: 10.1002/stc.253.

Péquegnat, C. et al., 2021, RÉSIF-SI: A Distributed Information System for French Seismological Data, Seismological Research Letters, 92, no. 3, 1832–1853, doi: 10.1785/0220200392.

Reuland, Y., P. Lestuzzi, and I. F. C. Smith, 2019, Measurement-based support for post-earthquake assessment of buildings, Structure and Infrastructure Engineering, 15, no. 5, 647–662, doi: 10.1080/15732479.2019.1569071.

Ritz, J.-F., S. Baize, M. Ferry, C. Larroque, L. Audin, B. Delouis, and E. Mathot, 2020, Surface rupture and shallow fault reactivation during the 2019 Mw 4.9 Le Teil earthquake, France, Commun Earth Environ, 1, no. 1, 10, doi: 10.1038/s43247-020-0012-z.

Ronald, J. A., A. Menon, A. M. Prasad, D. Menon, and G. Magenes, 2018, Modelling and analysis of South Indian temple structures under earthquake loading, Sādhanā, 43, no. 5, 74, doi: 10.1007/s12046-018-0831-0.

Roselli, I., M. Malena, M. Mongelli, N. Cavalagli, M. Gioffrè, G. De Canio, and G. de Felice, 2018, Health assessment and ambient vibration testing of the "Ponte delle Torri" of Spoleto during the 2016–2017 Central Italy seismic sequence, J. Civil Struct. Health Monit., 8, 199–216, doi: 10.1007/s13349-018-0268-5.

Saisi, A., C. Gentile, and A. Ruccolo, 2018, Continuous monitoring of a challenging heritage tower in Monza, Italy, J. Civil Struct. Health Monit., 8, no. 1, 77–90, doi: 10.1007/s13349-017-0260-5.

Sivori, D., M. Lepidi, and S. Cattari, 2020, Ambient vibration tools to validate the rigid diaphragm assumption in the seismic assessment of buildings, Earthquake Engng. Struct. Dyn., 49, no. 2, 194–211, doi: 10.1002/eqe.3235.

Todorovska, M. I., 2009, Soil-Structure System Identification of Millikan Library North-South Response during Four Earthquakes (1970-2002): What Caused the Observed Wandering of the System Frequencies?, Bulletin of the Seismological Society of America, 99, no. 2A, 626–635, doi: 10.1785/0120080333.

Ubertini, F., G. Comanducci, N. Cavalagli, A. L. Pisello, A. L. Materazzi, and F. Cotana, 2017, Environmental effects on natural frequencies of the San Pietro bell tower in Perugia, Italy, and their removal for structural performance assessment, Mechanical Systems and Signal Processing, 82, 307–322, doi: 10.1016/j.ymssp.2016.05.025.

Wu, W.-H., S.-W. Wang, C.-C. Chen, and G. Lai, 2017, Assessment of environmental and nondestructive earthquake effects on modal parameters of an office building based on long-term vibration measurements, Smart Mater. Struct., 26, 055034, doi: https://doi.org/10.1088/1361-665X/aa6ae6.

Zanotti Fragonara, L., G. Boscato, R. Ceravolo, S. Russo, S. Ientile, M. L. Pecorelli, and A. Quattrone, 2017, Dynamic investigation on the Mirandola bell tower in post-earthquake scenarios, Bull. Earthquake Eng., 15, no. 1, 313–337, doi: 10.1007/s10518-016-9970-z.